




On Irrotational Flows Beneath Periodic Traveling Equatorial Waves

Ronald Quirchmayr 

Communicated by A. Constantin

Abstract. We discuss some aspects of the velocity field and particle trajectories beneath periodic traveling equatorial surface waves over a flat bed in a flow with uniform underlying currents. The system under study consists of the governing equations for equatorial ocean waves within a non-inertial frame of reference, where Euler's equation of motion has to be suitably adjusted, in order to account for the influence of the earth's rotation.

Mathematics Subject Classification. 35Q35, 76B15.

Keywords. Surface waves, Coriolis effects, irrotational flows, particle paths.

1. Introduction

Irrotational flows of symmetric periodic traveling water waves over a flat bed are well-studied; from a theoretical point of view [4, 10, 19], numerically [1, 9, 11] and experimentally [23].

This paper deals with some qualitative properties of certain geophysical waves, which are not governed by Euler's equations of motion (which apply for inertial systems), but by suitable extensions that account for the influence of the earth's rotation. More precisely we study irrotational flows and particle paths beneath symmetric periodic traveling surface waves in regions close to the equator. In the case of equatorial surface waves, which propagate practically unidirectionally in the East–West direction due to the prevailing wind pattern (known as trade winds), it is justifiable¹ to consider the f -plane approximation for two-dimensional flows instead of the full geophysical governing equations in three dimensions. This reduction and the simplifying assumption of irrotationality,² implying that underlying currents are uniform, make it possible to analyze qualitative properties of the flow with the aid of well-known tools from complex and harmonic analysis, and conformal mapping theory. The qualitative techniques developed in [4, 10] to study Stokes waves can be adapted for the investigation of irrotational equatorial waves.

For recent studies of equatorial waves under the influence of the Coriolis effect we refer to [2, 3, 7, 8, 13, 14, 16, 18, 20, 22] and the references therein. In particular, the influence of the Coriolis force on the dispersion relation is brought to light in the papers [2, 13] dealing with surface waves; we refer moreover to [5] for effects on internal waves, and [17, 21] for edge waves.

The outline of the paper is the following. First we introduce the governing equations for equatorial waves in Sect. 2. After transforming this system to moving frame coordinates, we provide two alternative reformulations of the problem: a stream function formulation and its transformation on a strip via a conformal hodograph mapping. Section 3 is devoted to the study of the velocity field beneath a surface wave, which provides the basis for the qualitative description of particle trajectories in Sect. 4.

¹ We refer to the discussion in [7, 12].

² While non-uniform currents are prevalent in the equatorial ocean, these are typically subsurface currents. We treat gravity waves that are relevant for mean-surface flows.

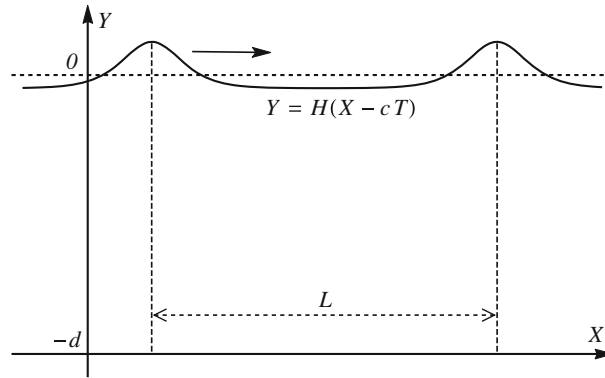


FIG. 1. The fluid domain $D_H(T)$ beneath a periodic traveling surface wave of wavelength L in the physical frame at some fixed time T

2. The Governing Equations for Equatorial Waves

The governing equations for gravity water waves in the equatorial f -plane are given by

$$\begin{cases} U_T + UU_X + VU_Y + 2\Omega V = -\frac{1}{\rho} \mathcal{P}_X \\ V_T + UV_X + VV_Y - 2\Omega U = -\frac{1}{\rho} \mathcal{P}_Y - g \\ U_X + V_Y = 0. \end{cases} \tag{2.1}$$

They hold in the domain $D_H(T) := \{(X, Y) \in \mathbb{R}^2 : -d < Y < H(X, T)\}$, where $H = H(X, T)$ parametrizes the free surface (Fig. 1). The velocity field is denoted by $(U, V) = (U(X, Y, T), V(X, Y, T))$, $P = P(X, Y, T)$ denotes the pressure, ρ is the constant fluid density, $g \approx 9.81 \text{ ms}^{-2}$ denotes the gravitational acceleration and $\Omega \approx 7.29 \times 10^{-5} \text{ rad s}^{-1}$ denotes the rotational speed of the earth. The boundary conditions associated with (2.1) on the free surface and the flat bed are given by

$$\begin{cases} \mathcal{P} = \mathcal{P}_{\text{atm}} \\ V = H_T + UH_X \end{cases} \quad \text{on } Y = H(X, T),$$

where \mathcal{P}_{atm} is the constant atmospheric pressure, and

$$V = 0 \quad \text{on } Y = -d.$$

We restrict our considerations on flows being irrotational at the initial time $T = 0$. The corresponding vorticity equation³ for such two-dimensional flows implies that the curl will remain zero for all times. We may therefore assume that (U, V) is curl-free throughout the fluid domain:

$$U_Y = V_X. \tag{2.2}$$

2.1. Moving Frame Re-formulation for Traveling Waves

The goal of this paper is the analysis of flows beneath traveling periodic surface waves. Let us therefore consider the corresponding moving frame coordinates for a given wave speed $c > 0$:

³ The details are provided in the Appendix.

$$\begin{aligned} x &:= X - cT, & y &:= Y \\ u(x, y) &:= U(X - cT, Y), & v(x, y) &:= V(x - cT, Y), \\ \eta(x) &:= H(X - cT), & P(x, y) &:= \frac{1}{\rho} \mathcal{P}(X - cT, Y), \end{aligned}$$

which transform (2.1) and (2.2) into

$$\begin{cases} (u - c)u_x + vu_y + 2\Omega v = -P_x \\ (u - c)v_x + vv_y - 2\Omega u = -P_y - g \end{cases} \tag{2.3}$$

$$u_x + v_y = 0 \tag{2.4}$$

$$u_y = v_x \tag{2.5}$$

in the fluid domain $D_\eta := \{(x, y) : -d < y < \eta(x)\}$. The corresponding boundary conditions on the free surface and on the flat bed are given by

$$v = (u - c)\eta_x \quad \text{on } y = \eta(x), \tag{2.6}$$

$$P = \frac{1}{\rho} \mathcal{P}_{\text{atm}} \quad \text{on } y = \eta(x), \tag{2.7}$$

and

$$v = 0 \quad \text{on } y = -d. \tag{2.8}$$

We assume that u, v, P and η are periodic in the x -direction. The period $L > 0$ corresponds to the wavelength of the surface wave.

2.2. Stream Function Formulation

Equation (2.4) permits the definition of a stream function satisfying

$$\psi_x = -v, \quad \psi_y = u - c. \tag{2.9}$$

We see that ψ is unique up to an additive constant and observe that ψ is constant on both parts of the boundary of D_η : on $y = -d$ due to (2.8) and also on the surface, since its derivative along the free surface η is zero by (2.6):

$$\partial_x(\psi(x, \eta(x))) = -v(x, \eta(x)) + (u(x, \eta(x)) - c)\eta_x(x) = 0.$$

With the choice

$$\psi = 0 \quad \text{on } y = \eta(x) \tag{2.10}$$

we obtain

$$\psi(x, y) = m + \int_{-d}^y (u(x, s) - c) ds \quad \text{for } -d \leq y \leq \eta(x).$$

This formula tells us in particular, that ψ inherits the x -periodicity from u . The constant m is called *relative mass flux*; its value is given by

$$m = \int_{-d}^{\eta(x)} (c - u(x, y)) dy. \tag{2.11}$$

Indeed, m is an invariant of the flow; differentiating the right hand side of (2.11) with respect to the x -variable and employing (2.4), (2.6) and (2.8) gives zero.

Due to (2.5) and (2.9) we obtain

$$\begin{pmatrix} (u - c)u_x + vu_y \\ (u - c)v_x + vv_y \end{pmatrix} = \begin{pmatrix} (u - c)u_x + vv_x \\ (u - c)u_y + vv_y \end{pmatrix} = \frac{1}{2} \nabla \psi_y^2 + \frac{1}{2} \nabla \psi_x^2$$

and

$$-2\Omega \begin{pmatrix} -v \\ u \end{pmatrix} = -2\Omega \nabla(\psi + cy).$$

Therefore (2.3) yields Bernoulli’s law for irrotational equatorial flows

$$\nabla \left(\frac{\psi_x^2 + \psi_y^2}{2} - 2\Omega(\psi + cy) + P + g(y + d) \right) = 0;$$

in other words, the expression

$$\frac{\psi_x^2 + \psi_y^2}{2} - 2\Omega(\psi + cy) + P + g(y + d) \tag{2.12}$$

is constant throughout the fluid. By means of (2.7) and (2.10) we infer that

$$\frac{\psi_x^2 + \psi_y^2}{2g} + \left(1 - \frac{2c\Omega}{g}\right)y + d = Q \quad \text{on } y = \eta(x)$$

for some physical constant Q , called *head*. In order to ensure positivity of the coefficient of y in the above relation, we impose the following realistic upper bound for the wave speed c :

$$c < \frac{g}{2\Omega}. \tag{2.13}$$

In summary we obtained the following reformulation of (2.3)–(2.8):

$$\begin{cases} \Delta\psi = 0 & \text{in } -d < y < \eta(x) \\ \psi = m & \text{on } y = -d \\ \psi = 0 & \text{on } y = \eta(x) \\ \frac{\psi_x^2 + \psi_y^2}{2g} + \left(1 - \frac{2c\Omega}{g}\right)y + d = Q & \text{on } y = \eta(x). \end{cases} \tag{2.14}$$

Note that the pressure P does not appear explicitly in (2.14). It can be recovered by means of (2.12) and (2.7):

$$P = gQ + \frac{1}{\rho} \mathcal{P}_{\text{atm}} - \frac{|\nabla\psi|^2}{2} + 2\Omega\psi - g \left[\left(1 - \frac{2c\Omega}{g}\right)y + d \right].$$

Since we are interested in solutions different from the trivial solution, that would be $\psi \equiv 0$ (with $m = 0$) throughout the strip D_0 , it follows from the strong maximum principle applied to the harmonic function ψ , that $m \neq 0$. Without loss of generality we take $m > 0$, then $\psi > 0$ throughout D_η and

$$\psi_y = u - c < 0 \quad \text{in } \bar{D}_\eta, \tag{2.15}$$

because ψ attains a minimum at every surface point $(x, \eta(x))$ and a maximum at every point $(x, -d)$ on the flat bad (by Hopf’s lemma, this strict inequality holds everywhere on the boundary ∂D_η of the fluid domain D_η , therefore the strong maximum principle applied on the harmonic function ψ_y implies (2.15)). The irrotationality condition (2.5) and L -periodicity imply that

$$0 = \int_{-d}^{y_0} \int_L^0 (u_y - v_x) \, dx \, dy = \int_0^L u(x, y_0) \, dx - \int_0^L u(x, -d) \, dx$$

at all depths y_0 below the trough level $\eta(L/2)$ by means of Green’s theorem. In other words: the mean of u at any depth below the trough level takes the constant value $\kappa < c$ referred to as *mean current*:

$$\kappa := \frac{1}{L} \int_0^L u(x, -d) \, dx = \frac{1}{L} \int_0^L u(x, y_0) \, dx \quad \text{for all } y_0 \in [-d, \eta(L/2)]. \tag{2.16}$$

We distinguish between three cases: if κ is positive, there is a uniform underlying current moving with the wave, if κ is negative, it moves against the wave and $\kappa = 0$ indicates the absence of an underlying current. In the latter case we have that:

$$\int_0^L u(x, -d) \, dx = 0. \tag{2.17}$$

An immediate consequence of (2.16) is that

$$\frac{1}{L} \int_0^L (u(x, -d) - c) \, dx = \kappa - c. \tag{2.18}$$

In the remaining sections we investigate flows beneath symmetric periodic traveling ocean waves. More precisely, we study qualitative properties of smooth periodic solutions (η, ψ) of (2.14) (for a given wave speed $c > 0$, relative muss flux $m > 0$ and mean current κ), having period L in the x -variable and mean level $y = 0$, i.e.

$$\int_0^L \eta(x) \, dx = 0.$$

Moreover η and ψ are supposed to be symmetric about the crest line, i.e. the vertical line from $(0, \eta(0))$ to $(0, -d)$, where η attains its maximum. Furthermore we assume that the surface wave η has only one crest per period. Its wave profile is supposed to be strictly increasing from the trough at $x = -L/2$, where the minimum is attained, to the crest at $x = 0$. In terms of the velocity field (u, v) and the pressure P , the symmetry of ψ means that u and P are symmetric, whereas v is anti-symmetric about the crest line. We refer the reader to [15] for the existence of solutions of (2.14) with these properties.

Let us note that the approach developed in [6] can be adapted to our setting for equatorial waves, yielding that the free surface is actually real-analytic.

2.3. Hodograph Transform

We introduce new coordinates q and p , which will turn out to be of great use in the further analysis.

Due to (2.5), there exists a potential ϕ for the velocity field $(u - c, v)$:

$$\phi_x = u - c, \quad \phi_y = v \tag{2.19}$$

We set

$$\phi(x, y) := \int_0^x (u(\xi, -d) - c) \, d\xi + \int_{-d}^y v(x, s) \, ds \tag{2.20}$$

for $-d \leq y \leq \eta(x)$. Then ϕ satisfies (2.19) and $\phi(0, y) = 0$ for all $y \in [-d, \eta(0)]$ since v is anti-symmetric about the crest line. Moreover, $\phi(L, y) = L(\kappa - c)$ for all y below the trough level by (2.16), whereas $\phi(-L, y) = -L(\kappa - c)$. The map $(x, y) \mapsto \phi(x, y) + (c - \kappa)x$ is odd and periodic in the x -variable with period L ; in particular $\phi(jL, y) = -(c - \kappa)jL$ for every integer j . Furthermore $\phi_x < 0$ by (2.15). Observe that

$$\phi(L/2, y_0) = -\frac{\lambda}{2} \quad \text{and} \quad \phi(-L/2, y_0) = \frac{\lambda}{2} \tag{2.21}$$

for all $y_0 \in [-d, \eta(L/2)]$, with $\lambda := L(c - \kappa)$, because the restrictions $u|_{(-L/2, 0)}$ and $u|_{(L/2, L)}$ coincide due to L -periodicity, hence

$$L\kappa = \int_0^L u(x, y_0) \, dx = \int_0^{L/2} u(x, y_0) \, dx + \int_{-L/2}^0 u(x, y_0) \, dx.$$

The two integrals on the right hand side are equal, since u is even, which gives (2.21).

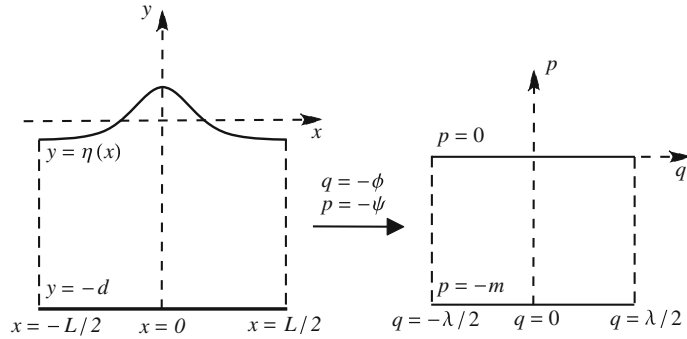


FIG. 2. The conformal hodograph transform maps the domain \overline{D}_η , which is an unknown part of the solution, to the closed strip between $p = 0$ and $p = -m$ by inverting the dependent and independent variables. The price is paid by a higher nonlinearity in the corresponding boundary condition

The stream function ψ and the potential ϕ are harmonic conjugates: the mapping $x + iy \mapsto \phi(x, y) + i\psi(x, y)$ is holomorphic throughout the fluid domain. Let us consider the orientation preserving conformal hodograph transform

$$\begin{cases} q = -\phi(x, y) \\ p = -\psi(x, y) \end{cases} \tag{2.22}$$

which transforms the free boundary value problem (2.14) into a nonlinear boundary value problem for the harmonic function

$$h(q, p) = y + d \tag{2.23}$$

in a fixed strip; c.f. Fig. 2. The corresponding system for h reads

$$\begin{cases} \Delta_{q,p} h = 0 & \text{in the strip } -m < p < 0 \\ h = 0 & \text{on } p = -m \\ \left(2g \left[\hat{Q} - \left(1 - \frac{2c\Omega}{g} \right) h \right] \right) (h_q^2 + h_p^2) = 1 & \text{on } p = 0 \end{cases} \tag{2.24}$$

where

$$\hat{Q} = Q - \frac{2c\Omega d}{g}. \tag{2.25}$$

We will frequently make use of the following identities:

$$\begin{aligned} \partial_q &= h_p \partial_x + h_q \partial_y \\ \partial_p &= -h_q \partial_x + h_p \partial_y \end{aligned} \tag{2.26}$$

$$\begin{aligned} \partial_x &= (c - u) \partial_q + v \partial_p \\ \partial_y &= -v \partial_q + (c - u) \partial_p \end{aligned} \tag{2.27}$$

$$\begin{aligned} h_q &= -\frac{v}{(u - c)^2 + v^2} = -\frac{\partial x}{\partial p} = \frac{\partial y}{\partial q} \\ h_p &= \frac{c - u}{(u - c)^2 + v^2} = \frac{\partial x}{\partial q} = \frac{\partial y}{\partial p} \end{aligned} \tag{2.28}$$

$$c - u = \frac{h_p}{h_q^2 + h_p^2}, \quad v = -\frac{h_q}{h_q^2 + h_p^2}. \tag{2.29}$$

Note for instance, that we obtained the boundary condition in (2.24) by multiplying the corresponding condition in (2.14) by $2g \frac{v^2 + (c-u)^2}{((c-u)^2 + v^2)^2}$ to get

$$1 = 2g \left[Q - \left(1 - \frac{2c\Omega}{g} \right) y + d \right] \frac{v^2 + (c-u)^2}{((c-u)^2 + v^2)^2} \quad \text{on } y = \eta(x).$$

This is precisely the boundary condition in (2.24) in view of (2.28), (2.23), (2.22), (2.25) and the fact, that $y = \eta(x)$ translates into $p = 0$ due to the definition of ψ .

3. Properties of the Velocity Field

This section is dedicated to the study of basic properties of the velocity field (u, v) of solutions (ψ, η) to (2.14) as we introduced them in the last paragraph of Sect. 2.2. In particular we will determine the zero level sets of u and v , where sign changes occur. This will permit a detailed qualitative analysis of fluid particle paths in the physical frame, see Sect. 4.

Due to periodicity we may restrict our considerations to the particular periodicity window

$$D := \{(x, y) : x \in (-L/2, 0), -d < y < \eta(x)\}.$$

We denote by \bar{D} the closure of D in \mathbb{R}^2 ; its left and right boundary⁴ are referred to as *trough lines*. The *crest line* is the intersection of \bar{D} with the vertical line $\{x = 0\}$. In view of the symmetry of ψ it is convenient to distinguish between the right half D_+ of D and its left half D_- :

$$\begin{aligned} D_+ &:= \{(x, y) : x \in (0, L/2), -d < y < \eta(x)\} \\ D_- &:= \{(x, y) : x \in (-L/2, 0), -d < y < \eta(x)\}. \end{aligned}$$

Let us furthermore denote by

$$\begin{aligned} S_+ &:= \{(x, y) : x \in (0, L/2), y = \eta(x)\} \\ S_- &:= \{(x, y) : x \in (-L/2, 0), y = \eta(x)\} \end{aligned}$$

and

$$\begin{aligned} B_+ &:= \{(x, y) : x \in (0, L/2), y = -d\} \\ B_- &:= \{(x, y) : x \in (-L/2, 0), y = -d\} \end{aligned}$$

the parts of the free surface and the flat bed, which correspond to D_+ and D_- respectively. We denote the images of D_- and D_+ under the conformal transformation of variables (2.22) by \hat{D}_- and \hat{D}_+ :

$$\begin{aligned} \hat{D}_- &:= \{(q, p) : -\frac{\lambda}{2} < q < 0, -m < p < 0\} \\ \hat{D}_+ &:= \{(q, p) : 0 < q < \frac{\lambda}{2}, -m < p < 0\}. \end{aligned}$$

We start our analysis by determining the sign of the vertical velocity component v in D , c.f. Fig. 3.

Proposition 3.1. *The vertical velocity component v is strictly positive in D_+ ; it is strictly negative in D_- and vanishes on the crest and trough lines.*

Proof. Recall that v is harmonic in the entire fluid domain; this is ensured by (2.4) and (2.5). Due to (2.6) and (2.15) we have that $v(x, \eta(x)) > 0$ for all $x \in (0, L/2)$, since $\eta'(x) < 0$ on this interval by assumption, c.f. the last paragraph of Sect. 2.2. Recall that $v = 0$ on the bottom. The strong maximum principle implies that $v > 0$ in D_+ , and since v is anti-symmetric we infer that $v < 0$ in D_- . By continuity we have that $v = 0$ on the crest line $x = 0$ and also on the trough lines $x \pm L/2$ in view of periodicity. \square

⁴ i.e. the sets $\bar{D} \cap \{x = -L/2\}$ and $\bar{D} \cap \{x = L/2\}$.

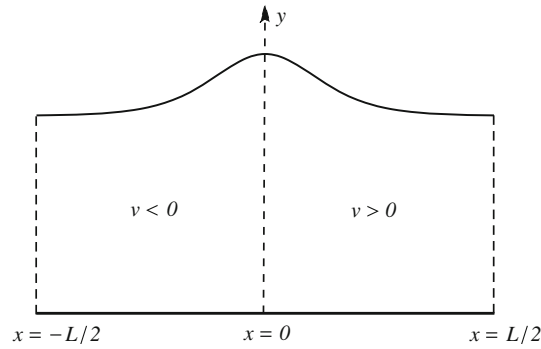


FIG. 3. The vertical component v of the velocity field is negative in the *left* half D_- of the periodicity window D , it is positive within the *right* half D_+ and vanishes on the crest line and both trough lines

As a consequence we obtain the following corollary, which tells us that all streamlines except the flat bed $y = -d$ replicate the shape of the free surface.

Corollary 3.2. *All streamlines $\{\psi = p\} \cap \bar{D}$ with $p \in (0, m)$, are analytic, symmetric and strictly decreasing between $x = 0$ and $x = L/2$.*

Proof. Recall that ψ has no critical points due to (2.15). Let us identify an arbitrary streamline in D with the function

$$y: (-L/2, L/2) \rightarrow \mathbb{R}, \quad x \mapsto y(x).$$

It is clear, that y is analytic, since it is a parametrization of a level set of the harmonic map ψ , i.e. $\psi(x, y(x))$ is constant for all $x \in (-L/2, L/2)$. Therefore we have that

$$0 = \partial_x(\psi(x, y(x))) = \psi_x(x, y(x)) + \psi_y(x, y(x))y_x$$

and hence

$$y_x(x) = \frac{v(x, y(x))}{u(x, y(x)) - c}.$$

Thus we see, in view of the sign of v together with (2.15), that all streamlines within D are symmetric and strictly decreasing between the wave crest and the wave trough. \square

Remark 3.3. Let y be a streamline in D . The continuous periodic continuation $\tilde{y}: \mathbb{R} \rightarrow \mathbb{R}$ to the entire fluid domain attains its maxima at crests and its minima at troughs, since \tilde{y}_x vanishes precisely on the crest and trough lines.

The next proposition reveals the monotonicity properties of the horizontal velocity component u along streamlines, the crest line and trough lines, c.f. Fig. 4.

Proposition 3.4. *The horizontal velocity component u is strictly decreasing along streamlines in $D_+ \cup S_+ \cup B_+$ and strictly increasing along streamlines in $D_- \cup S_- \cup B_-$; in particular⁵ $u_x = 0$ on the crest and trough lines. On the crest line it holds that $u_y > 0$, whereas $u_y < 0$ along the trough lines.*

Proof. Let us first observe that the pressure P is superharmonic throughout the entire fluid region, in particular within D . By (2.3) and (2.5) we have that

$$\begin{aligned} P_{xx} &= -u_x^2 - uu_{xx} + cu_{xx} - v_xu_y - vv_{yx} - 2\Omega v_x \\ &= -u_x^2 - uu_{xx} + cu_{xx} - v_x^2 - vv_{xx} - 2\Omega v_x \end{aligned}$$

⁵ In view of Corollary 3.2.

and

$$\begin{aligned} P_{yy} &= -u_y v_x - uv_{xy} + cv_{xy} - v_y^2 - vv_{yy} + 2\Omega u_y \\ &= -u_y^2 - uu_{yy} + cu_{yy} - u_x^2 - vv_{yy} + 2\Omega u_y, \end{aligned}$$

which sums up to

$$\begin{aligned} \Delta P &= P_{xx} + P_{yy} \\ &= -(v_x^2 + u_y^2) - 2u_x^2 - v\Delta v - u\Delta u + c\Delta u + 2\Omega(u_y - v_x). \end{aligned}$$

Therefore we obtain that

$$\Delta P = -(\psi_{xx}^2 + \psi_{yy}^2) - 2\psi_{xy}^2 \leq 0,$$

since both u and v are harmonic in the whole fluid domain by (2.4) and (2.5).

Let us now consider the function Q defined on the entire fluid domain and given by

$$Q(x, y) := P(x, y) - 2\Omega\psi(x, y).$$

The map Q is superharmonic as a sum of the superharmonic function P and a multiple of the harmonic function ψ . Therefore we have that the minimum of Q is attained on boundary of the fluid domain, i.e. on the flat bed or on the free surface. The maximum principle tells us that the minimum of Q is attained on the boundary of the fluid domain. On the bottom we find that

$$Q_y = P_y - 2\Omega u = -g + 2(\Omega - \Omega)u = -g < 0,$$

because of (2.8) and the second component of (2.3). Hence Q decreases in y -direction on the bottom, therefore the minimum can only be attained on the surface, where Q takes the constant value $\rho^{-1}\mathcal{P}_{\text{atm}}$; i.e. every point $(x, \eta(x))$ is a minimum point. Since the positive x -direction, as well as the positive y -direction, point outwards the fluid domain along S_+ we infer that both $Q_x(x, \eta(x))$ and $Q_y(x, \eta(x))$ are strictly negative for all $x \in (0, L/2)$. By (2.3) and the definition of Q we obtain

$$0 < -Q_x = (u(x, \eta(x)) - c)u_x(x, \eta(x)) + v(x, \eta(x))u_y(x, \eta(x))$$

for all $x \in (0, L/2)$. In terms of the (p, q) -coordinates this inequality reads

$$u_q(q, 0) = \frac{(c - u(x, \eta(x)))u_x(x, \eta(x)) - v(x, \eta(x))u_y(x, \eta(x))}{(c - u(x, \eta(x)))^2 + v(x, \eta(x))^2} < 0$$

for all $q \in (0, \lambda/2)$; here we employed (2.26).

Moreover, since $v = 0$ on the crest and trough lines, (2.4) guarantees that also $u_x = 0$ there and hence (2.26) tells us that

$$u_q(0, p) = u_q(\lambda/2, p) = 0 \quad \text{for } p \in [-m, 0].$$

On the flat bed we have that

$$u_q(q, -m) = \frac{u_x(x, -d)}{c - u(x, -d)} = -\frac{v_y(x, -d)}{c - u(x, -d)}.$$

Hopf's maximum principle yields that $v_y(x, -d) > 0$ for $x \in (0, L/2)$, since v is minimal along the bottom B_+ , and therefore we infer that

$$u_q(q, -m) < 0 \quad \text{for } q \in (0, \lambda/2).$$

In summary we have that $u_q \leq 0$ all along the boundary of \hat{D}_+ ; the inequality being strict on the upper and lower boundary. The harmonicity of u is preserved under (2.22), and so we can apply the strong maximum principle in order to find that

$$u_q < 0 \quad \text{throughout } \hat{D}_+. \tag{3.1}$$

Since u is even, we obtain that $u_q > 0$ in D_- . Thus we achieved the desired monotonicity along horizontal lines in the conformal frame, which correspond to streamlines in the moving frame. The transformation to

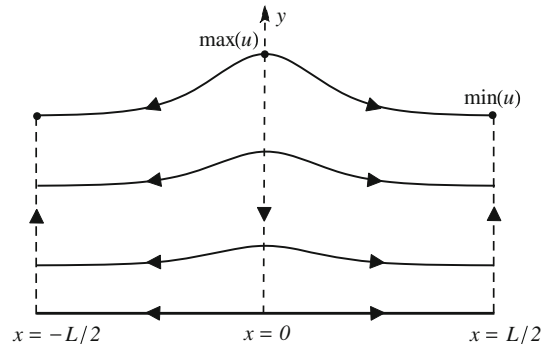


FIG. 4. An illustration of the assertions of Proposition 3.4, Corollaries 3.5 and 3.6. The monotonicity of the horizontal velocity component u along streamlines, the crest line and the trough lines is indicated by *arrows* pointing towards the directions of decrease. The maximum of u is attained on the crest, the troughs are minimizers of u

(x, y) -coordinates yields the claim: we know from the proof of Corollary 3.2 and (2.29) that the derivatives of parameterizations $y = y(x)$ of streamlines satisfy

$$\frac{dy}{dx} = \frac{v}{u - c} = \frac{h_q}{h_p},$$

hence (2.28) yields

$$\frac{\partial}{\partial x} [u(x, y(x))] = u_x + \frac{dy}{dx} u_y = u_x + \frac{h_q}{h_p} u_y = \frac{1}{h_p} u_q,$$

which determines the claimed monotonicity of u along streamlines, since $h_p > 0$ due to (2.28) and (2.15).

In order to establish the claimed monotonicity along the crest and trough lines we recall first that $u_y = (c - u)u_p$ on these lines because of (2.27) and the fact that v vanishes there due to Proposition 3.1. We recall that $u_p = v_q$ as a consequence of (2.4), (2.5) and (2.26). We recall from Proposition 3.1 that the harmonic function v is positive in D_+ and vanishes on the crest line and the trough lines, hence these points are minimizers of v in \bar{D}_+ . Therefore Hopf’s lemma tells us that

$$v_x(0, y) > 0 \quad \text{for } y \in (-d, \eta(0))$$

and

$$v_x(L/2, y) < 0 \quad \text{for } y \in (-d, \eta(L/2)).$$

The claim follows since $v_q = h_p v_x$ on the images of the crest and trough lines under the conformal mapping (2.22) and due to (2.15). □

Corollary 3.5. *The horizontal velocity component u attains its maximum at the wave crest $(0, \eta(0))$ and it is minimal at the wave troughs $(\pm L/2, \eta(\pm L/2))$.*

Proof. The maximum of u can only be attained somewhere along the crest line and its minimum has to be found on the trough lines, since $u_x < 0$ throughout the region

$$D_+ \cup S_+ \cup B_+$$

and $u_x > 0$ in

$$D_- \cup S_- B_-.$$

Due to Proposition 3.4 we know that u increases in y -direction on the crest line and decreases in y -direction on the trough lines, which proves the assertion of the corollary. □

Corollary 3.6. *The slopes of streamlines decrease in absolute value along vertical lines from the surface to the bottom.*

Proof. Recall first, that the slope of any streamline vanishes at crest and trough lines; see Remark 3.3. Let the functions $y: (-L/2, 0) \rightarrow \mathbb{R}, x \mapsto y(x)$ be the parameterizations of the restrictions of all streamlines to the left periodicity window \bar{D}_- . We want to compare their slopes $y'(x)$ at some fixed point $x \in (-L/2, 0)$. We have that $y'(x) = v(x, y)/(u(x, y) - c)$, (c.f. Corollary 3.2), where the y 's on the right hand side are understood to be the y -coordinates of the respective streamlines at the point x (i.e. $y \in [-d, \eta(x)]$). Then

$$\begin{aligned} \frac{\partial}{\partial y} \left[\frac{v(x, y)}{(u(x, y) - c)} \right] &= \frac{v_y(x, y)(u(x, y) - c) - u_y(x, y)v(x, y)}{(u(x, y) - c)^2} \\ &= \frac{u_x(x, y)(c - u(x, y)) - u_y(x, y)v(x, y)}{(u(x, y) - c)^2} > 0, \end{aligned}$$

because

$$u_q(q, p) = \frac{u_x(x, y)(c - u(x, y)) - u_y(x, y)v(x, y)}{(c - u(x, y))^2 + v^2} > 0$$

by Proposition 3.4. This proves the assertion for vertical lines intersecting $x \in (-L/2, 0)$, since the slopes of all streamlines are positive at such x , see Corollary 3.2. Likewise, $\frac{\partial}{\partial y} \left[\frac{v(x, y)}{(u(x, y) - c)} \right] < 0$ for $x \in (0, L/2)$, where all slopes are negative. \square

The monotonicity properties of the horizontal velocity component u allows a qualitative description of its zero-set $\{u = 0\}$. We discuss the special case without an underlying current in full detail in Proposition 3.7, c.f. the first image in Fig. 5. The general cases can be deduced from this case, see Remark 3.8.

Proposition 3.7. *If $\kappa = 0$, the zero-level-set of u in \bar{D} consists of a smooth curve \mathcal{C}_+ in D_+ and a smooth curve \mathcal{C}_- in D_- . Both \mathcal{C}_+ and \mathcal{C}_- connect the respective parts B_+ and B_- of the flat bed with the corresponding surface parts S_+ and S_- and intersect each streamline exactly at one point. They separate \bar{D} into the three regions where u has a sign: u is strictly positive in the set between \mathcal{C}_+ and \mathcal{C}_- and strictly negative in the corresponding complement with respect to \bar{D} .*

Proof. Recall that (2.16) implies, c.f. (2.21), that

$$\int_0^{L/2} u(x, -d) dx = 0.$$

Since $u_x(x, -d) < 0$ for all $x \in (0, L/2)$, there exists a unique $x_0 \in (0, L/2)$ such that $u(x_0, -d) = 0$. This implies the existence of a unique $q_0 \in (0, \lambda/2)$ such that $u(q_0, -m) = 0$. Strict monotonicity of u on the bottom between 0 and $\lambda/2$ implies that $u(q, -m) > 0$ for $q \in [0, q_0)$ and $u(q, -m) < 0$ for $q \in (q_0, \lambda/2]$. By combining the inequality $u(0, -m) > 0 > u(\lambda/2, -m)$ with the monotonicity along the crest and trough lines, see Proposition 3.4, we obtain

$$u(0, p) > 0 > u(\lambda/2, p) \quad \text{for } p \in [-m, 0]. \tag{3.2}$$

From (3.1) and (3.2) we infer that u vanishes exactly once along the intersections of horizontal lines with \hat{D}_+ . These line segments correspond to the intersections of level sets of ψ with D_+ which represent (parts of) the stream lines of the velocity field in the moving frame. The corresponding pictures for the domain \hat{D}_- and D_- are obtained by reflecting \hat{D}_+ and D_+ at the vertical lines $\{q = 0\}$ and $\{x = 0\}$ respectively. Let us denote by $(\hat{\alpha}(p), p), p \in (-m, 0)$ the path of points in \hat{D}_+ where u vanishes. Due to (3.1) we may apply the implicit function theorem at every point $(\hat{\alpha}(p), p)$ and can thereby reconstruct the map $p \mapsto \hat{\alpha}(p)$ globally as a smooth curve $\hat{\mathcal{C}}_+$. The pre-image of this curve under the coordinate transform (2.22) is a smooth curve \mathcal{C}_+ in D_+ , parametrized by $(\alpha(y), y)$, that connects the flat bed $y = -d$ with the free surface $y = \eta(x)$ by intersecting each streamline exactly once. \square

Remark 3.8 (Sign of \mathbf{u} in flows with an underlying current). This case can be traced back to the case $\kappa = 0$: let (ψ, η) be a symmetric L -periodic solution to (2.14) representing the wave speed $c > 0$, relative mass flux $m > 0$ and mean current κ . We may identify (ψ, η) with (ψ_0, η_0) which represents an L -periodic

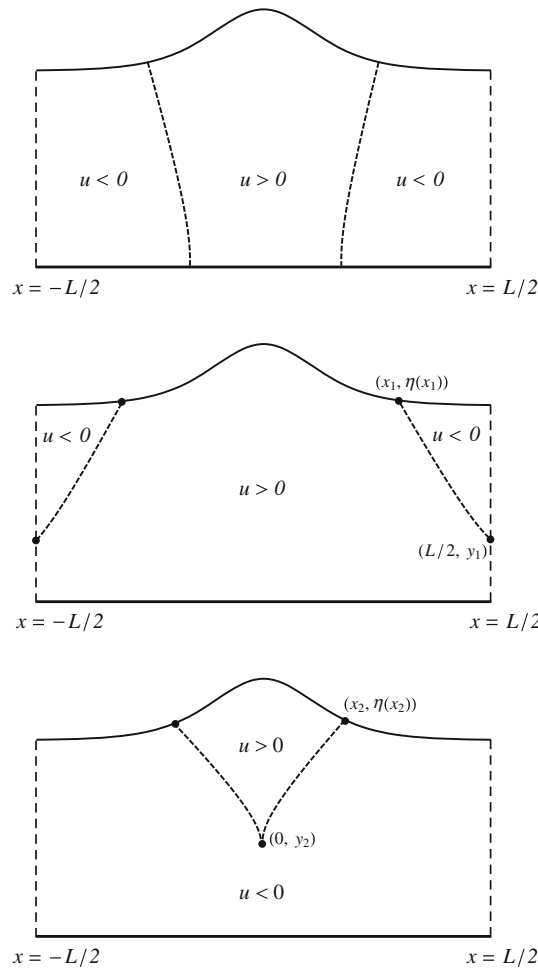


FIG. 5. The *dashed curves* are the zero sets of u , which separate \bar{D} into parts of positive and negative sign. The image on the *top* illustrates the case without or with a weak favorable or weak adverse current, the *second picture* shows the scenario of a moderate favorable current and the *last image* explains the situation of a moderate adverse current

solution for the wave speed $c_0 = c - \kappa > 0$ *without* the presence of an underlying current; namely via taking $u_0 = u - \kappa, v_0 = v, \eta_0 = \eta$ (and $\psi_0 = \psi$, since $u_0 - c_0 = u - c$). Then $u_0 < c_0$ is guaranteed. We distinguish between the cases $\kappa > 0$ and $\kappa < 0$, which are divided into three sub-cases:⁶

1. $\kappa > 0$.
 - (a) $\kappa \leq -u_0(L/2, -d)$. This situation matches qualitatively the case $\kappa = 0$: there is exactly one sign change of u somewhere on the flat bed. In the borderline case $u(L/2, -d) = 0$, the set $\{u = 0\}$ connects the point $(L/2, -d)$ with some surface point $(x_0, \eta(x_0))$, where $0 < x_0 < L/2$.
 - (b) $-u_0(L/2, -d) < \kappa < -u_0(L/2, \eta(L/2))$. Here, the curve $\{u = 0\}$, connects a point $(L/2, y_1)$ on the trough line with some surface point $(x_1, \eta(x_1))$, $0 < x_1 < L/2$.
 - (c) $\kappa \geq -u_0(L/2, \eta(L/2))$. In this case, u is nonnegative throughout \bar{D}_+ , i.e. no change of sign occurs.

⁶ We describe the situation for D_+ ; the picture for D_- is obtained by reflection about the y -axis. The observations rely on the strict monotonicity of u along streamlines in $D_+ \cup S_+ \cup B_+$ and its monotonicity in y -direction along the crest and trough line, c.f. Proposition 3.4 and the proof of Proposition 3.7.

2. $\kappa < 0$.⁷

- (a) $-u_0(0, -d) \leq \kappa$. As in (1a), the situation matches qualitatively the case $\kappa = 0$. In the borderline case $u(0, -d) = 0$, the smooth zero-set $\{u = 0\}$ connects the point $(0, -d)$ with some surface point $(x_1, \eta(x_1))$, where $0 < x_1 < L/2$.
- (b) $-u_0(0, \eta(0)) < \kappa < -u_0(0, -d)$. The curve $\{u = 0\}$ connects a point $(0, y_2)$ on the crest line with some surface point $(x_2, \eta(x_2))$, $0 < x_2 < L/2$.
- (c) $-\frac{g}{2\Omega} + c < \kappa \leq -u_0(0, \eta(0))$. Similar as in (1c), no change of sign occurs: $u \leq 0$ throughout \bar{D}_+ .

4. The Particle Path Pattern

In this section we study the trajectory $t \mapsto (X(t), Y(t))$ of a fluid particle initially located at (X_0, Y_0) , which satisfies the system

$$\begin{cases} X' = U(X - cT, Y) \\ Y' = V(X - cT, Y) \end{cases} \tag{4.1}$$

with initial condition $(X(0), Y(0)) = (X_0, Y_0)$. In the moving frame the above time dependent problem is transformed to the autonomous system

$$\begin{cases} x' = u(x, y) - c \\ y' = v(x, y) \end{cases} \tag{4.2}$$

with initial data $(x(0), y(0)) = (X_0, Y_0)$. We note that ψ is a Hamiltonian for this system, i.e. ψ satisfies

$$\begin{cases} x' = \partial_y \psi \\ y' = \partial_x \psi \end{cases}$$

and moreover ψ is an integral of motion,

$$\psi(x(t), y(t)) = \psi(X_0, Y_0) \quad \text{for all } t \in \mathbb{R}, \tag{4.3}$$

since it does not depend on time.

Let us assume, that the fluid particle is initially (at time $t = 0$) located at the point $(L/2, Y_0)$ and observe that this is no restriction of the general case, since any fluid particle would cross the vertical line $\{x = L/2\}$ after some finite time in view of the moving frame. Indeed, due to (2.15) and (4.2) there exists a $\delta > 0$ such that $x' = u(x, y) - c \leq -\delta < 0$ for all (x, y) in the entire fluid domain, and this means that x runs from ∞ to $-\infty$ when t goes from $-\infty$ to ∞ . Since u is periodic in x , there exists a uniquely determined positive time (depending only on the initial height Y_0) it takes a fluid particle to traverse one periodicity window of length L :

Definition 4.1. The time $\tau = \tau(Y_0) > 0$ which satisfies $x(\tau) = -L/2$ is called the *elapsed time*.

Remark 4.2 (Viewpoint q, p -coordinates). Let us denote by $(q(t), p(t))$ the images of points $(x(t), y(t))$ under the conformal transformation of variables (2.22) and recall that $p(t) = p$ is an integral of motion because of (2.22) and (4.3), whereas

$$\frac{dq}{dt} = -\frac{d\phi}{dt} = -\phi_x x' - \phi_y y' = -(c - u)^2 - v^2 \leq \delta^2$$

by (2.19) and (4.2). So $(q(t), p(t))$ moves along straight horizontal lines from right to left in the (q, p) -plane. This shows (by keeping in mind that $q(0) = \lambda/2$) that there exists a unique time $\theta = \theta(p)$ such

⁷ Note that we require $-\kappa < \frac{g}{2\Omega} - c$ to ensure that c_0 satisfies (2.13).

that $q(\theta) = -\lambda/2$. By construction we have that θ coincides with the elapsed time: $\theta(p) = \tau(Y_0)$ and consistently we obtain

$$\begin{aligned} y(\tau) - y(0) &= \int_0^\tau v(x(t), y(t)) \, dt \\ &= \int_0^\theta p'(t) \, dt = \int_{-\lambda/2}^{\lambda/2} -h_q(q, p) \, dq \\ &= \int_{-\lambda/2}^{\lambda/2} \frac{v}{(c-u)^2 + v^2} \, dq = 0, \end{aligned}$$

where the last equality holds true because v is odd in the q -variable.

Proposition 4.3. *The elapsed time is given by*

$$\theta(p) = \int_{-L/2}^{L/2} \frac{dx}{c - u(x, y_{Y_0}(x))} = \int_{\lambda/2}^{\lambda/2} [h_q^2(q, p) + h_p^2(q, p)] \, dq \tag{4.4}$$

and satisfies

$$\theta(p) > \frac{L}{c - \kappa} \quad \text{for all } p \in [-m, 0]. \tag{4.5}$$

Proof. Let us first consider the case $p \neq 0$, i.e. $Y_0 \neq -d$. By parameterizing the particular streamline containing the point $(L/2, Y_0)$ via the map $x \mapsto y_{Y_0}(x), y_{Y_0}: [-L/2, L/2] \rightarrow \mathbb{R}$, we may write the elapsed time $\theta(p)$ as

$$\theta(p) = \int_0^\theta 1 \, dt = \int_0^\theta \frac{x'(t)}{u(x(t), y(t)) - c} \, dt = \int_{-L/2}^{L/2} \frac{dx}{c - u(x, y_{Y_0}(x))}. \tag{4.6}$$

In order to recognize the second representation of θ we recall that

$$h_p^2 + h_q^2 = \frac{1}{(c - u)^2 + v^2}$$

by means of (2.28), and calculate the derivative of q along streamlines:

$$\frac{dq}{dx} = -\frac{d}{dx} [\phi(x, y(x))] = c - u(x) + \frac{v(x)^2}{c - u(x)} = \frac{(c - u(x))^2 + v(x)^2}{c - u(x)}.$$

Let us now consider the divergence-free vector field $(v, c-u)$ (recall (2.5)) restricted to the region $D_{y_{Y_0}} \subseteq \bar{D}$ beneath the streamline $y = y_{Y_0}(x)$, above the flat bed $y = -d$ and between the trough lines $x = \pm L/2$. The divergence theorem implies that

$$\begin{aligned} 0 &= \int_{\partial D_y} (v, c - u) \cdot \mathbf{n} \, dS \\ &= \int_{-L/2}^{L/2} (u(x, -d) - c) \, dx + \int_{-L/2}^{L/2} (c - u(x, y_{Y_0}(x))) \sqrt{1 + (\partial_x y_{Y_0}(x))^2} \, dx, \end{aligned} \tag{4.7}$$

where we exploited the anti-symmetry of v and the fact that y_{Y_0} has the same shape as the free surface, see Corollary 3.2. By exploiting (2.21) and the periodicity of u in the x -variable, we infer from (4.7) that

$$(c - \kappa)L = \int_{-L/2}^{L/2} (c - u(x, y_{Y_0}(x))) \sqrt{1 + (\partial_x y_{Y_0}(x))^2} \, dx. \tag{4.8}$$

Due to the Cauchy–Schwarz inequality we get

$$\begin{aligned}
 L^2 &= \left(\int_{-L/2}^{L/2} \sqrt{\frac{c - u(x, y_{Y_0}(x))}{c - u(x, y_{Y_0}(x))}} dx \right)^2 \\
 &\leq \int_{-L/2}^{L/2} \frac{dx}{c - u(x, y_{Y_0}(x))} \int_{-L/2}^{L/2} (c - u(x, y_{Y_0}(x))) dx.
 \end{aligned}
 \tag{4.9}$$

We recall that the streamline y_{Y_0} satisfies (see Corollary 3.2)

$$\partial_x y_{Y_0}(x) \neq 0 \quad \text{for } x \in (-L/2, L/2) \setminus \{0\},$$

and hence

$$\int_{-L/2}^{L/2} (c - u(x, y_{Y_0}(x))) \sqrt{1 + (\partial_x y_{Y_0}(x))^2} dx > \int_{-L/2}^{L/2} (c - u(x, y_{Y_0}(x))) dx.
 \tag{4.10}$$

In summery we get from (4.6), (4.9), (4.10) and (4.8) that

$$\begin{aligned}
 \theta(p) &= \int_{-L/2}^{L/2} \frac{dx}{c - u(x, y(x))} dx \geq \frac{L^2}{\int_{-L/2}^{L/2} (c - u(x, y(x))) dx} \\
 &> \frac{L^2}{\int_{-L/2}^{L/2} (c - u(x, y(x))) \sqrt{1 + (\partial_x y_{Y_0}(x))^2} dx} = \frac{L^2}{(c - \kappa)L} = \frac{L}{c - \kappa}
 \end{aligned}$$

for all $p \in (-m, 0]$.

In order to see that $\theta(p) > L/(c - \kappa)$ holds still true for $p = -m$, we argue by contradiction: if we assume the contrary, namely that $\theta(-m) = L/(c - \kappa)$, we enforce equality in the Cauchy-Schwarz inequality (4.7):

$$L^2 = \int_{-L/2}^{L/2} \frac{dx}{c - u(x, -d)} \int_{-L/2}^{L/2} (c - u(x, -d)) dx,$$

which means that the functions $x \mapsto \frac{1}{c - u(x, -d)}$ and $x \mapsto (c - u(x, -d))$ are linearly dependent. But this would only be possible if u was constant on the flat bed, but this is not the case, since we know that $u_x < 0$ on $(0, L/2)$ by Proposition 3.4. And so we conclude that (4.5) is satisfied. \square

Proposition 4.4. *The elapsed time $\theta(p)$ decreases strictly with depth $p \in [-m, 0]$.*

Proof. We show that $\theta'(-m) = 0$ and $\theta''(p) > 0$ for $p \in (-m, 0]$. Differentiation of (4.4) with respect to p gives

$$\theta' = 2 \int_{\lambda/2}^{\lambda/2} [h_q h_{qp} + h_p h_{pp}] dq.$$

Since h is periodic the q -variable with period λ , we obtain

$$0 = \int_{\lambda/2}^{\lambda/2} (h_q h_p)_q dq = \int_{\lambda/2}^{\lambda/2} [h_q h_{qp} + h_p h_{qq}] dq$$

for all $p \in [-m, 0]$; therefore the fact that h is harmonic yields that

$$\theta' = 4 \int_{\lambda/2}^{\lambda/2} h_p h_{pp} dq = -4 \int_{\lambda/2}^{\lambda/2} h_p h_{qq} dq$$

for all $p \in [-m, 0]$, in particular we get that

$$\theta'(-m) = 0
 \tag{4.11}$$

, since h_q is constantly zero on the flat bed by (2.8). The second derivative of θ is given by

$$\theta'' = 4 \int_{\lambda/2}^{\lambda/2} [h_{pp}^2 + h_p h_{ppp}] dq = 4 \int_{\lambda/2}^{\lambda/2} [h_{pp}^2 + h_{pq}^2] dq \geq 0 \tag{4.12}$$

for all $p \in [-m, 0]$; in order to establish the second equality, we used once more, that h is harmonic and λ -periodic in q :

$$0 = \int_{\lambda/2}^{\lambda/2} (h_p h_{ppq})_q dq = \int_{\lambda/2}^{\lambda/2} [h_{pq}^2 + h_p h_{ppq}] dq = \int_{\lambda/2}^{\lambda/2} [h_{pq}^2 - h_p h_{ppp}] dq.$$

Combining (4.11) and (4.12) yields $\theta' \geq 0$ for all $p \in [-m, 0]$. Finally we show that the inequality is strict on $(-m, 0]$. Assuming the contrary, namely that $\theta'(p_0) = 0$ for some $p_0 \in (-m, 0]$, monotonicity of θ' implies that $\theta'(p) = 0$ for all $p \in [-m, p_0]$, yielding that $\theta'' = 0$ on $[-m, 0]$. Then (4.12) implies that $h_{pq} = h_{pp} = 0$ in $[-\lambda/2, \lambda/2] \times [-m, p_0]$, and thus h_p is constant throughout this rectangle. By recalling that $h_p = (c - u)^{-1}$ on the lower boundary $p = -m$ by (2.28) and (2.8), this contradicts Proposition 3.4. \square

Definition 4.5. The *particle drift* $\mathfrak{D} = \mathfrak{D}(Y_0)$ is the net horizontal distance that a particle moves in the physical frame until the elapsed time passes by:

$$\mathfrak{D} := X(\tau) - X(0).$$

Proposition 4.6. *A particle path is closed if and only if $\mathfrak{D} = 0$.*

Proof. If a particle trajectory is closed, there exists some time $T > 0$ such that $(X(T), Y(T)) = (X_0, Y_0)$. From $Y(T) = Y_0$ it follows that $T = n\theta$ for some nonzero integer n . Then it holds that $0 = X(n\tau) - X(0) = n(X(\tau) - X(0))$ which implies that $\mathfrak{D}(Y_0) = 0$.

If on the other hand $\mathfrak{D}(Y_0) = 0$, then $X(\tau) = X(0), Y(\tau) = Y(0)$ and $\tau = L/c$. By x -periodicity both $t \mapsto (X(t), Y(t))$ and $t \mapsto (X(t+\tau), Y(t+\tau))$ solve (4.1) with the initial condition $(X(0), Y(0)) = (X_0, Y_0)$. Since (U, V) is real analytic and bounded, thus in particular Lipschitz continuous, we have uniqueness of solutions, i.e. $X(t + \tau) = X(t)$ and $Y(t + \tau) = Y(t)$ for all $t \in \mathbb{R}$. \square

Proposition 4.7. *The particle drift \mathfrak{D} satisfies*

$$\mathfrak{D}(p) = c\theta(p) - L > \frac{cL}{c - \kappa} - L \quad \text{for all } p \in [-m, 0]. \tag{4.13}$$

In particular, the drift is strictly positive for each fluid particle, if $\kappa \geq 0$.

Proof. We have that $X(T) = x(t) + ct$, and in time τ the solution $(x(t), y(t))$ of (4.2) moves by definition from the trough line $x = L/2$ to the next trough line $x = -L/2$ in the moving frame. Hence $X(0) = x(0) = L/2, X(\tau) = x(\tau) + c\tau$ and thus $X(\tau) - X(0) = -L + c\tau = c\theta - L$. The estimate in (4.13) is due to Proposition 4.3. \square

As an immediate consequence of Propositions 4.6 and 4.7, we obtain the following

Corollary 4.8. *If $\kappa \geq 0$, the particle drift $\mathfrak{D}(p)$ is positive for all $p \in [-m, 0]$; in particular, there are no closed particle paths.*

Moreover, Propositions 4.4 and 4.7 yield

Corollary 4.9. *The particle drift $\mathfrak{D}(p)$ decreases strictly with depth $p \in [-m, 0]$.*

We collect all possible scenarios concerning the sign of the particle drift in case of a negative κ in the following

Remark 4.10 (Sign of the drift in the case of an adverse current). If $\kappa < 0$, the particle drift \mathfrak{D} can either have the same (positive or negative) sign everywhere in D , or there exists a streamline \mathcal{Y} of zero drift in D , where \mathfrak{D} changes sign (from positive to negative, when going from the surface S to the bed B across \mathcal{Y} , according to Corollary 4.9). To be more precise, let κ_B and κ_S be the values of the adverse current,

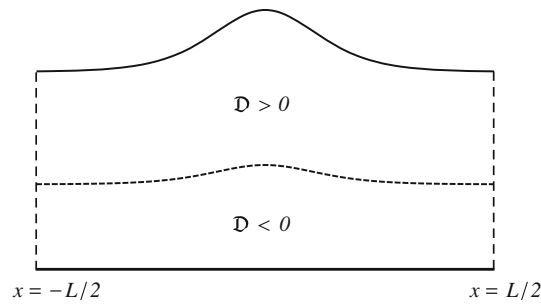


FIG. 6. The case of an adverse current with the property $\kappa_S < \kappa < \kappa_B$ is characterized by the existence of a streamline which contains the particles having zero drift. It separates D into an *upper part* where the drift is positive, and a *lower region*, where it is negative

for which the drift vanishes on B and S respectively. In view of the notation introduced in Remark 3.8 and the formula (4.13) for the particle drift, we have that

$$\kappa_B = \frac{L}{\theta(-m)} - c_0 \quad \text{and} \quad \kappa_S = \frac{L}{\theta(0)} - c_0, \tag{4.14}$$

where

$$\theta(-m) = \int_{-L/2}^{L/2} \frac{dx}{c - u(x, -d)} = \int_{-L/2}^{L/2} \frac{dx}{c_0 - u_0(x, -d)} > \frac{L}{c_0} \tag{4.15}$$

and

$$\theta(0) = \int_{-L/2}^{L/2} \frac{dx}{c - u(x, \eta(x))} = \int_{-L/2}^{L/2} \frac{dx}{c_0 - u_0(x, \eta(x))} > \frac{L}{c_0} \tag{4.16}$$

due to Proposition 4.3. Therefore, as desired, both κ_B and κ_S are negative. Additionally, Corollary 4.9 tells us that

$$\kappa_S < \kappa_B < 0.$$

So in view of the strict monotonicity of the particle drift $\mathcal{D}(p)$, see Corollary 4.9, we end up with the following cases.

1. $\kappa_B \leq \kappa < 0$. The drift is positive from the surface S down to the bed B . In the borderline case $\kappa = \kappa_B$, we have that $\mathcal{D}(p) > 0$ for $p \in (-m, 0]$ and $\mathcal{D}(-m) = 0$.
2. $\kappa_S < \kappa < \kappa_B$. In this situation, $\mathcal{D}(0) > 0$ and $\mathcal{D}(-m) < 0$, thus Corollary 4.9 yields the existence of a unique streamline \mathcal{Y} in D where \mathcal{D} vanishes (along which particles move in circles due to Proposition 4.6), and the drift becomes negative for particles below \mathcal{Y} (Fig. 6).
3. $-\frac{g}{2\Omega} + c < \kappa \leq \kappa_S$. The drift is negative from the surface to the bed. In the borderline situation $\kappa = \kappa_S$ it holds that $\mathcal{D}(p) < 0$ for $p \in [-m, 0)$ and $\mathcal{D}(0) = 0$.

We exploit now the insights gained from studying the velocity field in Sect. 3 and the particle drift to describe the particle trajectories in a qualitative manner. The discussion contains the three different scenarios of no underlying current ($\kappa = 0$), a favorable current ($\kappa > 0$) and an adverse current ($\kappa < 0$).

4.1. Particle Trajectories in Flows Without Underlying Currents

In the situation of the absence of an underlying current, we proved (see Proposition 3.7) that the level set $\{u = 0\}$ in D_+ consists of a smooth curve \mathcal{C}_+ , which connects B_+ with S_+ and intersects each streamline $\{\psi = -p\}$ with $p \in [-m, 0]$ exactly once. The corresponding curve \mathcal{C}_- that represents the level set $\{u = 0\}$ in D_- is obtained by reflecting \mathcal{C}_+ in the vertical line $\{x = 0\}$.

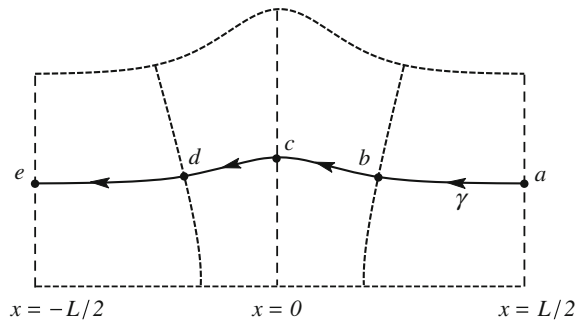


FIG. 7. The trajectory γ in the moving frame intersects the trough lines in points a, e , and crest line in c , where v changes the sign, and the points b and d , where u changes the sign

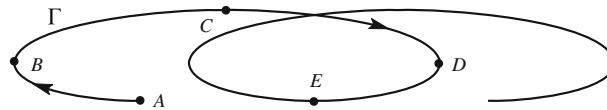


FIG. 8. The path Γ in the physical frame corresponds to the trajectory γ in the moving frame, and the points A, B, C, D, E correspond to a, b, c, d, e respectively; c.f. Fig. 7

Let us distinguish between the position $(x(t), y(t))$ of the particle at time t in the moving frame and the corresponding position $(X(t), Y(t))$ in the physical frame. Let $\gamma = \gamma_{Y_0} : [0, \theta] \rightarrow \mathbb{R}^2, t \mapsto (x(t), y(t))$ be the trajectory of the particle in the moving frame (Fig. 7) and let $\Gamma = \Gamma_{Y_0} : [0, \theta] \rightarrow \mathbb{R}^2, t \mapsto (X(t), Y(t))$ be the corresponding path in the physical frame (Fig. 8).

As before we assume that the particle is initially located at

$$a = (x(0), y(0)) = (L/2, Y_0) = (X(0), Y(0)) = A.$$

Let b, c, d be the points, where γ intersects \mathcal{C}_+ , the crest line $\{x = 0\}$, and the curve \mathcal{C}_- respectively, and let us denote by $e = \gamma(\theta(Y_0)) = (-L/2, Y_0)$ the endpoint of γ . Let I_{ab} be the open time interval while $(x(t), y(t))$ is located between a and b ; the time intervals I_{bc}, I_{cd} and I_{de} are defined analogously. Furthermore let B, C, D and E be the corresponding points in the physical frame. We have that $E = \Gamma(\theta) = (-L/2 + c\theta, Y_0)$ lies to the right of A since $\mathfrak{D}(Y_0) > 0$. Since the images $\gamma(I_{ab})$ and $\gamma(I_{de})$ lie within regions where $u < 0$, the corresponding horizontal displacement $\Gamma(t)$ has to be backwards during these time intervals. The image $\gamma(I_{bd})$ lies in the region where $u > 0$, hence $\Gamma(t)$ moves forward during this time interval. Moreover $\gamma(I_{ac})$ lies in D_+ , where v is strictly positive, thus $\Gamma(t)$ moves upwards within the time window I_{ac} and $\Gamma(t)$ moves downwards for $t \in I_{ce}$ since $\gamma(I_{ce})$ lies in D_- , where v is strictly negative. This description holds for all particles being initially located above the flat bed.

A particle which is initially located on the flat bed, i.e. $Y_0 = -d$, will always remain there, since $v = 0$. We have that $\Gamma_{-d}(t)$ moves forward at times $t \in I_{bd}$, it moves backwards when t lies in the time intervals I_{ab} and I_{de} . This means that the particle oscillates backward–forward–backward, mirroring the projection of the loops of $\Gamma_{Y_0}, Y_0 > -d$ to the flat bed.

4.2. Particle Trajectories in Favorable Currents

As in the previous case, the drift is positive for all particles; see Proposition 4.7. We recall that the sign of the vertical velocity component v is not effected by the presence of an underlying current, see Proposition 3.1. We only have to take into account the qualitative changes of the horizontal velocity component u for an increasing mean current κ in order to give a qualitative description of the motion of fluid particles. According to Remark 3.8, we distinguish three different cases, regarding the sign of u in \bar{D} .

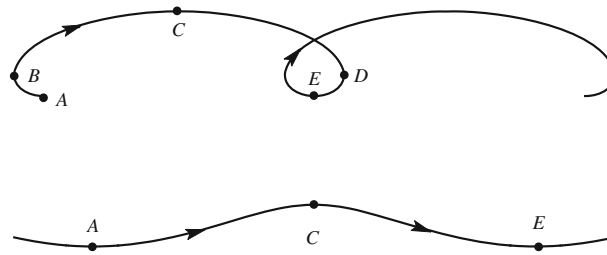


FIG. 9. Particle paths in the presence of a favorable current: the *first* trajectory corresponds to that of a particle experiencing a small favorable current or that of a particle in a moderate one above the critical streamline \mathcal{Y} (the loops are smaller in comparison with Fig. 8), the *second* describes the wavelike path on or below \mathcal{Y} , or that of the particles experiencing a strong favorable current

In the case of a small favorable current, where $\kappa \leq -u_0(L/2, -d)$, the particle path pattern is the same as in the case $\kappa = 0$. Only in the borderline case $\kappa = -u_0(L/2, -d)$ the situation changes for particles at the flat bed: there is no backward motion at all.

In the case of a moderate favorable current, where one finds that $-u_0(L/2, -d) < \kappa < -u_0(L/2, \eta(L/2))$, the qualitative picture of the particle paths depends on the depth: a critical streamline \mathcal{Y} separates \bar{D} into two layers. Particles in the upper layer follow the $\kappa = 0$ pattern, whereas particles on or below \mathcal{Y} do not move backwards.

If $\kappa \geq -u_0(L/2, \eta(L/2))$, we say that a strong favorable current is present and all particles experience a pure forward motion.

Particles which are located at the flat bed move to the right with a periodic change of velocity in the latter two sub-cases.

We visualized our considerations in Fig. 9.

4.3. Particle Trajectories in Adverse Currents

In the situation of an adverse current, the possibility of a negative particle drift has to be taken additionally into account in order to describe particle paths. We combine the results in Remarks 3.8 and 4.10 to classify the particle path pattern.

First we observe, that Proposition 3.4 on the monotonicity of u together with (4.14), (4.15) and (4.16) allow us to relate $\kappa_S, \kappa_B, -u_0(0, \eta(0))$ and $-u_0(0, -d)$:

$$-u_0(0, \eta(0)) < \kappa_S \quad \text{and} \quad -u_0(0, -d) < \kappa_B;$$

we keep also in mind that $\kappa_S < \kappa_B$ as well as $-u_0(0, \eta(0)) < -u_0(0, -d)$. Note that in general we can not determine a priori, whether $\kappa_S < -u_0(0, -d)$ or $-u_0(0, -d) \leq \kappa_S$. Therefore the following scenarios for the motion of particles might occur when an adverse current is present.

1. $\kappa_B \leq \kappa$. The drift is still positive (it vanishes on the bottom, if $\kappa = \kappa_B$), and u changes its sign periodically along every streamline. The qualitative picture is the same as in the $\kappa = 0$ case, c.f. Fig. 8.
2. $\kappa_S < \kappa < \kappa_B$ and $-u_0(0, -d) \leq \kappa$. The sign of the drift alters across a certain streamline \mathcal{Y} and u still changes sign along every streamline (if $\kappa = -u_0(0, -d)$, u is negative on $B \setminus \{(0, -d)\}$, entailing a pure backward motion which stagnates only in bottom points directly below the crest). The particles on \mathcal{Y} move clockwise on a closed path, c.f. Fig. 10. Particles above \mathcal{Y} are looping to the right, below \mathcal{Y} they are looping to the left, c.f. Fig. 11.
3. $-u_0(0, -d) \leq \kappa \leq \kappa_S$. The drift is negative for all particles (except for surface particles in the case $\kappa = \kappa_S$, in which $\mathcal{D}(0) = 0$ and surface particles move on closed paths) and u behaves as in the previous scenario, hence particles are looping to the left.
4. $\kappa_S < \kappa < -u_0(0, -d)$. There is a zero drift streamline \mathcal{Y}_1 , that separates D into an upper region of positive drift and a lower region of negative drift, along which particles move on closed paths. And

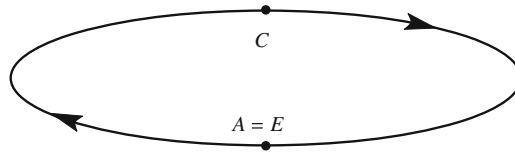


FIG. 10. A closed particle trajectory on a zero-drift streamline

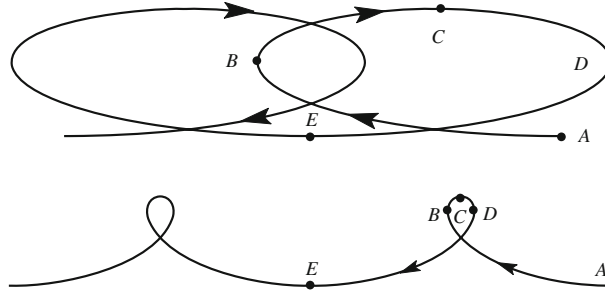


FIG. 11. The trajectories of two different particles looping to the left: the distance from A to E depends on κ and the depth of the particle's initial position

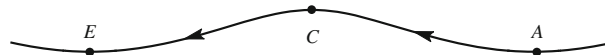


FIG. 12. A fluid particle moving wavelike to the left

there is a streamline \mathcal{Y}_2 which splits D into an upper region, where u changes signs, and a lower region, where u is negative. Observe, that it can not happen, that \mathcal{Y}_1 lies below \mathcal{Y}_2 , since this would entail particles with a pure backward motion but a positive drift. Moreover it is not possible, that \mathcal{Y}_1 and \mathcal{Y}_2 coincide: closed loops enforce a periodic occurrence of backward and forward motion. Therefore \mathcal{Y}_1 lies above \mathcal{Y}_2 , and D splits into three different layers. In the lowest one, particles move wavelike to the left, c.f. Fig. 12. Particles in the middle layer are looping to the left, and particles in the top layer are looping to the right.

5. $\kappa < \kappa_S$ and $-u_0(0, \eta(0)) < \kappa < -u_0(0, -d)$. The drift is negative for all particles and there exists a streamline \mathcal{Y} that splits D into an upper layer, where u changes sign along streamlines, and a lower layer, where u is negative. Particles in the upper layer loop to the left, whereas particles below \mathcal{Y} move as depicted in Fig. 12.
6. $c - \frac{g}{2\Omega} < \kappa \leq -u_0(0, -d)$. Here both \mathfrak{D} and u are negative throughout D . All particles move wavelike to the left.

Remark 4.11. We have demonstrated that the movement of particles within irrotational flows beneath periodic traveling equatorial surface waves follows the same qualitative pattern as it is the case for Stokes waves; c.f. the results in [4, 10]. We could essentially reproduce these results for irrotational equatorial waves. Let us point out once again, that the bounds we have imposed on c and κ are not restrictive from a physical point of view.

Nevertheless, it is remarkable, that even in the presence of Coriolis effects in the f -plane, we can preserve the analysis without any restrictions on the wave amplitude; in particular our results do not rely on approximations.

Let us finally point out, that the effects of underlying (uniform) currents on particle paths in our setting is quite different from that in the explicit equatorial waves obtained in [2, 5, 13, 16, 17, 21] for flows

with non-constant vorticity. These papers start by imposing a circular particle path in the absence of a current, changed to a trochoid by an underlying current, whereas in our setting for irrotational flows, closed particle paths are only possible, if there is a suitable adverse current.

Appendix A. Vorticity Equation for Equatorial Waves

We provide a derivation of the vorticity equation for three-dimensional flows beneath equatorial waves, which describes the evolution of the vorticity in a flow.

Let us for this purpose denote the velocity field by

$$u(x, t) = (u_1(x, t), u_2(x, t), u_3(x, t))$$

and the (scalar) pressure field by $P(x, t)$, where $x = (x_1, x_2, x_3)$ are the spacial coordinates and t is the time in the physical frame. Henceforth the gradient reads $\nabla = (\partial_{x_1}, \partial_{x_2}, \partial_{x_3})$, furthermore the symbol “ \times ” denotes the cross product in \mathbb{R}^3 and “ \cdot ” denotes the scalar product.

With this notation and by setting the density $\rho = 1$ for notational convenience, the governing equations for equatorial waves in the f -plane read

$$\begin{cases} u_t + (u \cdot \nabla)u + 2\Omega(u_3, 0, -u_1) = -\nabla(P + gz) \\ \nabla \cdot u = 0. \end{cases} \quad (\text{A.1})$$

We apply the vector identity $(u \cdot \nabla)u = \nabla(1/2 u \cdot u) + (\nabla \times u) \times u$ on the first equation of (A.1) and denote by $\omega = (\nabla \times u)$ the vorticity to obtain

$$u_t + \omega \times u + 2\Omega(u_3, 0, -u_1) = -\nabla(1/2 u \cdot u + P + gz). \quad (\text{A.2})$$

Next we apply $\nabla \times$ on (A.2), use the identity

$$\nabla \times (a \times b) = (b \cdot \nabla)a - (a \cdot \nabla)b + a(\nabla \cdot b) - b(\nabla \cdot a)$$

for continuously differentiable vector fields a, b in \mathbb{R}^3 , and get

$$\omega_t + (u \cdot \nabla)\omega - (\omega \cdot \nabla)u + \omega(\nabla \cdot u) - u(\nabla \cdot \omega) - 2\Omega\partial_{x_2}u = 0.$$

Since the divergence of ω is generally zero and due to the second equation (conservation of mass) in (A.1), we end up with the vorticity equation

$$\frac{D\omega}{Dt} = (\omega \cdot \nabla)u + 2\Omega\partial_{x_2}u. \quad (\text{A.3})$$

Here, $D/Dt = \partial/\partial t + (u \cdot \nabla)$ denotes the so-called material derivative.

For the special situation of a two-dimensional flow, which can be identified with a three dimensional flow satisfying $u_2 = 0$ with u_1 and u_3 being independent of the x_2 -variable, it holds that $(\omega \cdot \nabla)u = \omega_2\partial_{x_2}u = 0$, and therefore equation (A.3) reads

$$\frac{D\omega}{Dt} = 0.$$

This means, that the local spin of each fluid particle is preserved, as it moves with the flow. In particular, particles having no local spin at the initial time, will never acquire it.

Acknowledgments. Open access funding provided by University of Vienna. The author is grateful for helpful comments from both referees. The support of the Austrian Science Fund (FWF), Grant W1245, is acknowledged.

Open Access. This article is distributed under the terms of the Creative Commons Attribution 4.0 International License (<http://creativecommons.org/licenses/by/4.0/>), which permits unrestricted use, distribution, and reproduction in any medium, provided you give appropriate credit to the original author(s) and the source, provide a link to the Creative Commons license, and indicate if changes were made.

References

- [1] Chen, Y.-Y., Hsu, H.-C., Chen, G.-Y.: Lagrangian experiment and solution for irrotational finite-amplitude progressive gravity waves at uniform depth. *Fluid Dyn. Res.* **42**, Art. No. 045511 (2010)
- [2] Constantin, A.: An exact solution for equatorially trapped waves. *J. Geophys. Res. Oceans* **117**, Art. No. C05029 (2012)
- [3] Constantin, A.: On the modelling of equatorial waves. *Geophys. Res. Lett.* **39**, Art. No. L05602 (2012)
- [4] Constantin, A.: The trajectories of particles in Stokes waves. *Invent. Math.* **166**, 523–535 (2006)
- [5] Constantin, A.: Some nonlinear, equatorially trapped, nonhydrostatic internal geophysical waves. *J. Phys. Oceanogr.* **44**, 781–789 (2014)
- [6] Constantin, A., Escher, J.: Analyticity of periodic travelling free surface water waves with vorticity. *Anal. Math.* **173**, 589–568 (2011)
- [7] Constantin, A., Johnson, R.S.: The dynamics of waves interacting with the equatorial undercurrent. *Geophys. Astrophys. Fluid. Dyn.* **109**, 311–358 (2015)
- [8] Constantin, A., Johnson, R.S.: An exact, steady, periodic, purely azimuthal equatorial flow with a free surface. *J. Phys. Oceanogr.* doi:[10.1175/JPO-D-15-0205.1](https://doi.org/10.1175/JPO-D-15-0205.1) (in press)
- [9] Constantin, A., Kalimeris, K., Scherzer, O.: A penalization method for calculating the flow beneath traveling water waves of large amplitude. *SIAM J. Appl. Math.* **75**, 1513–1535 (2015)
- [10] Constantin, A., Strauss, W.: Pressure beneath a Stokes wave. *Commun. Pure Appl. Math.* **63**, 533–557 (2010)
- [11] Clamond, D.: Note on the velocity and related fields of steady irrotational two-dimensional surface gravity waves. *Phil. Trans. R. Soc. A* **370**, 1572–1586 (2012)
- [12] Fedorov, A.V., Brown, J.N.: Equatorial waves. In: Steele, J. (ed.) *Encyclopedia of Ocean Sciences*, Academic Press, New York (2009)
- [13] Henry, D.: An exact solution for equatorial geophysical water waves with an underlying current. *Eur. J. Mech. B Fluids* **38**, 18–21 (2013)
- [14] Henry, D.: Internal equatorial water waves in the f -plane. *J. Nonlinear Math. Phys.* **22**, 499–506 (2015)
- [15] Henry, D., Mاتيoc, A.-V.: On the symmetry of steady equatorial wind waves. *Nonlinear Anal. Real World Appl.* **18**, 50–56 (2014)
- [16] Hsu, H.-C.: An exact solution for equatorial waves. *Monatsh. Math.* **176**, 143–152 (2015)
- [17] Ionescu-Kruse, D.: An exact solution for geophysical equatorial edge waves in the β -plane approximation. *J. Math. Fluid Mech.* **17**, 699–706 (2015)
- [18] Johnson, R.S.: An ocean undercurrent, a thermocline, a free surface, with waves: a problem in classical uid mechanics. *J. Nonlinear Math. Phys.* **22**, 475–493 (2015)
- [19] Kogelbauer, F.: Symmetric irrotational water waves are traveling waves. *J. Differ. Equ.* **259**, 5271–5275 (2015)
- [20] Martin, C.L.: Dynamics of the thermocline in the equatorial region of the Pacific ocean. *J. Nonlinear Math. Phys.* **22**, 516–522 (2015)
- [21] Mاتيoc, A.-V.: An exact solution for geophysical equatorial edge waves over a sloping beach. *J. Phys. A* **45**, Art. No. 365501 (2012)
- [22] Quirchmayr, R.: On the existence of benthic storms. *J. Nonlinear Math. Phys.* **22**, 540–544 (2015)
- [23] Umeyama, M.: Eulerian–Lagrangian analysis for particle velocities and trajectories in a pure wave motion using particle image velocimetry. *Phil. Trans. R. Soc. A* **370**, 1687–1702 (2012)

Ronald Quirchmayr
 Faculty of Mathematics
 University of Vienna
 Oskar-Morgenstern-Platz 1
 1090 Wien, Austria
 e-mail: ronald.quirchmayr@univie.ac.at

(accepted: July 13, 2016; published online: August 6, 2016)